Published Ahead of Print on August 1, 2019, as doi:10.3324/haematol.2019.219550.

haematologica
Journal of The Ferrata Storti Foundation

Biological and clinical implications of BIRC3 mutations in chronic lymphocytic leukemia

by Fary Diop, Riccardo Moia, Chiara Favini, Elisa Spaccarotella, Lorenzo De Paoli, Alessio Bruscaggin, Valeria Spina, Lodovico Terzi-di-Bergamo, Francesca Arruga, Chiara Tarantelli, Clara Deambrogi, Silvia Rasi, Ramesh Adhinaveni, Andrea Patriarca, Simone Favini, Sruthi Sagiraju, Clive Jabangwe, Ahad A. Kodipad, Denise Peroni, Francesca R. Mauro, Ilaria Del Giudice, Francesco Forconi, Agostino Cortelezzi, Francesco Zaja, Riccardo Bomben, Francesca Maria Rossi, Carlo Visco, Annalisa Chiarenza, Gian Matteo Rigolin, Roberto Marasca, Marta Coscia, Omar Perbellini, Alessandra Tedeschi, Luca Laurenti, Marina Motta, David Donaldson, Phil Weir, Ken Mills, Patrick Thornton, Sarah Lawless, Francesco Bertoni, Giovanni Del Poeta, Antonio Cuneo, Antonia Follenzi, Valter Gattei, Renzo Luciano Boldorini, Mark Catherwood, Silvia Deaglio, Robin Foá, Gianluca Gaidano, and Davide Rossi

Haematologica 2019 [Epub ahead of print]

Citation: Fary Diop, Riccardo Moia, Chiara Favini, Elisa Spaccarotella, Lorenzo De Paoli, Alessio Bruscaggin, Valeria Spina, Lodovico Terzi-di-Bergamo, Francesca Arruga, Chiara Tarantelli, Clara Deambrogi, Silvia Rasi, Ramesh Adhinaveni, Andrea Patriarca, Simone Favini, Sruthi Sagiraju, Clive Jabangwe, Ahad A. Kodipad, Denise Peroni, Francesca R. Mauro, Ilaria Del Giudice, Francesco Forconi, Agostino Cortelezzi, Francesco Zaja, Riccardo Bomben, Francesca Maria Rossi, Carlo Visco, Annalisa Chiarenza, Gian Matteo Rigolin, Roberto Marasca, Marta Coscia, Omar Perbellini, Alessandra Tedeschi, Luca Laurenti, Marina Motta, David Donaldson, Phil Weir, Ken Mills, Patrick Thornton, Sarah Lawless, Francesco Bertoni, Giovanni Del Poeta, Antonio Cuneo, Antonia Follenzi, Valter Gattei, Renzo Luciano Boldorini, Mark Catherwood, Silvia Deaglio, Robin Foá, Gianluca Gaidano, and Davide Rossi. Biological and clinical implications of BIRC3 mutations in chronic lymphocytic leukemia.
Haematologica. 2019; 104:xxx
doi:10.3324/haematol.2019.219550

Biological and clinical implications of *BIRC3* mutations in chronic lymphocytic leukemia

Fary Diop,[1*] Riccardo Moia,[1*] Chiara Favini,[1] Elisa Spaccarotella,[1] Lorenzo De Paoli,[1] Alessio Bruscaggin,[2] Valeria Spina,[2] Lodovico Terzi-di-Bergamo,[2] Francesca Arruga[3], Chiara Tarantelli[4], Clara Deambrogi,[1] Silvia Rasi,[1] Ramesh Adhinaveni,[1] Andrea Patriarca,[1] Simone Favini,[1] Sruthi Sagiraju,[1] Clive Jabangwe[1], Ahad A. Kodipad,[1] Denise Peroni,[1] Francesca R. Mauro,[5] Ilaria Del Giudice,[5] Francesco Forconi,[6,7] Agostino Cortelezzi,[8] Francesco Zaja,[9] Riccardo Bomben,[10] Francesca Maria Rossi, [10] Carlo Visco,[11] Annalisa Chiarenza,[12] Gian Matteo Rigolin,[13] Roberto Marasca,[14] Marta Coscia,[15] Omar Perbellini,[16] Alessandra Tedeschi,[17] Luca Laurenti,[18] Marina Motta,[19] David Donaldson,[20] Phil Weir,[20] Ken Mills,[21] Patrick Thornton,[22] Sarah Lawless[20], Francesco Bertoni[4], Giovanni Del Poeta,[23] Antonio Cuneo,[13] Antonia Follenzi,[24] Valter Gattei,[10] Renzo Luciano Boldorini,[25] Mark Catherwood,[20] Silvia Deaglio,[3] Robin Foà,[5] Gianluca Gaidano[1°] and Davide Rossi[2°]

*FR and RM equally contributed to the study; °GG and DR equally contributed

[1]Division of Hematology, Department of Translational Medicine, Amedeo Avogadro University of Eastern Piedmont, Novara, Italy; [2]Institute of Oncology Research and Oncology Institute of Southern Switzerland, Bellinzona, Switzerland; [3]Department of Medical Sciences, University of Turin & Italian Institute for Genomic Medicine, Turin, Italy; [4]Università della Svizzera italiana, Institute of Oncology Research, Bellinzona, Switzerland; [5]Hematology, Department of Cellular Biotechnologies and Hematology, Sapienza University, Rome, Italy; [6]Cancer Sciences Unit, Southampton Cancer Research UK and National Institute for Health Research Experimental Cancer Medicine Centre, University of Southampton, Southampton, United Kingdom; [7]Division of Hematology, University of Siena, Siena, Italy; [8]Department of Hematology Oncology, Foundation IRCCS Ca' Granda Ospedale Maggiore Policlinico and University of Milan, Milan, Italy; [9]Clinica Ematologica, DAME, University of Udine, Udine, Italy; [10]Clinical and Experimental Onco-Hematology Unit, Centro di Riferimento Oncologico, Istituto di Ricovero e Cura a Carattere Scientifico (IRCCS), Aviano, Italy; [11]Department of Cell Therapy and Hematology, Ospedale San Bortolo, Vicenza, Italy; [12]Division of Hematology, Azienda Ospedaliera Universitaria Policlinico-OVE, Catania, Italy; [13]Hematology Section, Azienda Ospedaliero Universitaria Arcispedale S. Anna, University of Ferrara, Ferrara, Italy; [14]Division of Hematology, Department of Oncology and Hematology, University of Modena and Reggio Emilia, Modena, Italy; [15]Division of Hematology, Azienda Ospedaliero Universitaria Città della Salute e della Scienza and University of Turin, Turin, Italy; [16]Section of Hematology, Department of Medicine, University of Verona, Verona, Italy; [17]Department of Oncology/Haematology, Niguarda Cancer Center, Niguarda Ca Granda Hospital, Milan, Italy; [18]Fondazione Policlinico Universitario A. Gemelli, Rome, Italy; [19]Department of Hematology, Spedali Civili, Brescia, Italy; [20]Clinical Haematology, Belfast City Hospital, Belfast Health and Social Care Trust, Belfast, Northern Ireland; [21]Centre for Cancer Research and Cell Biology (CCRCB), Queen's University Belfast, Belfast, Northern Ireland, United Kingdom; [22]Department of Haematology, Beaumont Hospital, Dublin; [23]Department of Hematology, Tor Vergata University, Rome, Italy; [24]Department of Health Sciences, University of Eastern Piedmont Amedeo Avogadro, Novara, Italy; Department of Pathology, University of Eastern Piedmont Amedeo Avogadro, Novara, Italy.

Correspondence: Davide Rossi, MD, PhD, Hematology, Oncology Institute of Southern Switzerland and Institute of Oncology Research, 6500 Bellinzona, Switzerland; Ph +41 91 820 03 62; Fax +41 91 820 03 97; E-mail davide.rossi@eoc.ch; Gianluca Gaidano, MD, PhD, Division of Hematology, Department of Translational Medicine, Amedeo Avogadro University of Eastern Piedmont, Via Solaroli 17, 28100 Novara, Italy; Ph +39-0321-660655; Fax +39-0321-620421; E-mail gianluca.gaidano@med.uniupo.it.

Aknowledgments: This work was supported by: Molecular bases of disease dissemination in lymphoid malignancies to optimize curative therapeutic strategies, (5 x 1000 No. 21198), Associazione Italiana per la Ricerca sul Cancro Foundation, Milan, Italy (to GG and RF); Progetti di Rilevante Interesse Nazionale

(PRIN), (2015ZMRFEA), Rome, Italy; Partially funded by the AGING Project – Department of Excellence – DIMET, Università del Piemonte Orientale, Novara, Italy; Partially funded by Novara AIL ONLUS, Novara, Italy; Associazione Italiana per la Ricerca sul Cancro (AIRC IG-17314); Swiss cancer League, ID HSR-4660-11-2018, Bern, Switzerland; Research Advisory Board of the Ente Ospedaliero Cantonale, Bellinzona, Switzerland; European Research Council (ERC) Consolidator Grant CLLCLONE ID: 772051; Grant No. 320030_169670/1 Swiss National Science Foundation, Berne, Switzerland; Fondazione Fidinam, Lugano, Switzerland; Nelia & Amadeo Barletta Foundation, Lausanne, Switzerland; Fond'Action, Lausanne, Switzerland.

ABSTRACT

BIRC3 is a recurrently mutated gene in chronic lymphocytic leukemia but the functional implications of *BIRC3* mutations are largely unexplored. Also, little is known about the prognostic impact of *BIRC3* mutations in chronic lymphocytic leukemia cohorts homogeneously treated with first line fludarabine, cyclophosphamide, and rituximab. By immunoblotting analysis, we showed that the non-canonical NF-κB pathway is active in *BIRC3* mutated cell lines and in primary chronic lymphocytic leukemia samples, as documented by the stabilization of MAP3K14 and by the nuclear localization of p52. In addition, *BIRC3* mutated primary chronic lymphocytic leukemia cells are less sensitive to fludarabine. In order to confirm in patients that *BIRC3* mutations confer resistance to fludarabine-based chemoimmunotherapy, a retrospective multicenter cohort of 287 untreated patients receiving first-line fludarabine, cyclophosphamide, and rituximab was analyzed by targeted next generation sequencing of 24 recurrently mutated genes in chronic lymphocytic leukemia. By univariate analysis adjusted for multiple comparisons *BIRC3* mutations identify a poor prognostic subgroup of patients failing fludarabine, cyclophosphamide, and rituximab (median progression free survival: 2.2 years, $p < 0.001$) similar to cases harboring *TP53* mutations (median progression free survival: 2.6 years, $p < 0.0001$). *BIRC3* mutations maintained an independent association with an increased risk of progression with a hazard ratio of 2.8 (95% confidence interval 1.4-5.6, $p = 0.004$) in multivariate analysis adjusted for *TP53* mutation, 17p deletion and *IGHV* mutation status. If validated, *BIRC3* mutations may be used as a new molecular predictor to select high-risk patients for novel frontline therapeutic approaches.

INTRODUCTION

Nuclear factor-κB (NF-κB) signaling is a key component of chronic lymphocytic leukemia (CLL) development and evolution.[1] Two NF-κB pathways exist namely, canonical and non-canonical.[2] The former is triggered by the B-cell receptor (BCR) signaling via the Bruton's tyrosine kinase (BTK), while the latter is activated by members of the tumor necrosis factor (TNF) cytokine family.[3] Upon receptor binding, the TRAF3/MAP3K14-TRAF2/BIRC3 negative regulatory complex of non-canonical NF-κB signaling is disrupted, MAP3K14 (also known as NIK), the central activating kinase of the pathway, is released and activated to induce the phosphorylation and proteasomal processing of p100, thereby leading to the formation of p52-containing NF-κB dimers. The p52 protein dimerizes with RelB to translocate into the nucleus, where it regulates gene transcription. BIRC3 is a negative regulator of non-canonical NF-κB. Physiologically, BIRC3 (also known as cIAP2) catalyzes MAP3K14 protein ubiquitination in a manner that is dependent on the E3 ubiquitinine ligase activity of its C-terminal RING domain. MAP3K14 ubiquitination results into its proteasomal degradation.[4]

B-cell neoplasia often pirates signaling pathways by molecular lesions to promote survival and proliferation. Though according to bioinformatics criteria *BIRC3* is one of the candidate driver genes of CLL, the functional implications of *BIRC3* mutations are partially unexplored.[5-7] Also, little is known about the prognostic impact of *BIRC3* mutations in CLL cohorts homogeneously treated with first line fludarabine, cyclophosphamide, and rituximab (FCR).[7]

FCR is the most effective chemoimmunotherapy regimen for the management of CLL in young and fit patients devoid of *TP53* disruption.[8] Survival after FCR, however, is variable, and is affected by the molecular characteristics of the CLL clone.[9] Deletion of 17p and *TP53* mutations capture most, but not all patients who are refractory to chemo-immunotherapy, which prompts the identification of additional biomarkers associated with early failure of FCR.[10-12]

METHODS

Functional studies

The human CLL cell line MEC1, the splenic marginal zone lymphoma (SMZL) cell lines SSK41 and VL51, the mantle cell lymphoma (MCL) cell lines MAVER-1, Z-138 and JEKO-1, the human HEK-293T cell line, as well as primary CLL cells were used in functional experiments. The entire non-canonical NF-κB pathway was assessed by Western blot. Quantitative real-time PCR (qRT-PCR) was utilized to analyze the non-canonical NF-κB signature. Primary CLL were exposed to fludarabine and venetoclax for 24-48 hours and apoptosis measured using the eBioscience Annexin V Apoptosis Detection Kit APC (ThermoFisher). Details are supplied in the Supplementary Methods.

Cancer personalized profiling by deep sequencing (CAPP-seq)

A retrospective multicenter cohort of 287 untreated CLL receiving first-line therapy with FCR was analyzed for mutations, including 173 patients derived from a previously published multicenter clinical series and 114 new patients not included in our previous report.[10] The study was approved by the Ethical Committee of the Ospedale Maggiore della Carità di Novara associated with the Amedeo Avogadro University of Eastern Piedmont (study number CE 67/14). Further information is supplied in the Supplementary Methods. A targeted resequencing gene panel was designed to include: *i*) coding exons plus splice site of 24 genes known to be implicated in CLL pathogenesis and/or prognosis; *ii*) 3'UTR of *NOTCH1*; and *iii*) enhancer and promoter region of *PAX5* (size of the target region: 66627bp) (Table S1).[6,7] The next generation sequencing (NGS) libraries for genomic DNA (gDNA) were constructed using the KAPA Library Preparation Kit (Kapa Biosystems) and NGS libraries for RNA were constructed using RNA Hyper Kit (Roche). Multiplexed libraries (n = 10 per run) were sequenced using 300-bp paired-end runs on a MiSeq sequencer (Illumina) to obtain a coverage of at least 2000x in >90% of the target region (66627bp)

in 80% of cases (Table S2). A robust and previously validated bioinformatics pipeline was used for variant calling (Supplemental Appendix).

Statistical analysis

Progression free survival (PFS) was the primary endpoint. Survival analysis was performed by Kaplan-Meier method and compared between strata using the Log-rank test. To account for multiple testing, adjusted p-values were calculated using the Bonferroni correction. The adjusted association between exposure variables and PFS was estimated by Cox regression. Internal validation of the multivariate analysis was performed using a bootstrap approach. Statistical significance was defined as p value < 0.05 (Supplemental Appendix).

RESULTS

BIRC3 mutations associate with activation of non-canonical NF-κB signaling

In order to comprehensively map unique *BIRC3* mutations in CLL, we compiled somatically confirmed variants identified in the current CLL study cohort with those identified in previous studies[13] or listed in public CLL mutation catalogues (Figure 1 A). Virtually all *BIRC3* mutations were represented by frameshift or stop codons clustering in two hotspot regions comprised between amino acid 367-438 and amino acid 537-564. *BIRC3* variants were predicted to generate aberrant truncated transcripts causing the elimination or truncation of the C-terminal RING domain of the BIRC3 protein. The RING domain of BIRC3 harbors the E3 ubiquitin ligase activity that is essential for proteasomal degradation of MAP3K14, the central activating kinase of the non-canonical NF-κB signaling. This observation points to non-canonical NF-κB activation through MAP3K14 stabilization as the predicted functional consequence of *BIRC3* mutations in CLL.

The non-canonical NF-κB signaling was profiled by immunoblotting in B-cell tumor cell lines and primary CLL cells with different genetic make-up in the non-canonical NF-κB pathway to verify whether *BIRC3* mutations lead to constitutive non-canonical NF-κB activation. Additional genetic features of the above mentioned cell lines and primary CLL cells are shown in Table S3. In the VL51 SMZL cell line and in the MEC1 CLL cell lines, both harboring endogenous truncating mutations of the *BIRC3* gene, non-canonical NF-κB signaling was constitutively active, as documented by the stabilization of MAP3K14, phosphorylation of NF-κB_2, its processing from p100 to p52, as well as nuclear localization of p52 (Figure 1 B-D). Consistent with the biochemical clues of non-canonical NF-κB activation, the gene expression signature of the VL51 and MEC1 cell lines was significantly enriched of non-canonical NF-κB target genes (Figure 1 E-F). Non-canonical NF-κB signaling in *BIRC3* mutated cells was consistent with that of MCL cell lines known to harbor a disrupted TRAF3/MAP3K14-TRAF2/BIRC3 negative regulatory complex by loss of TRAF3 or TRAF2.[14] As *BIRC3* mutated cell lines, also primary CLL samples harboring inactivating mutations of *BIRC3* showed stabilization of MAP3K14 and NF-κB_2 processing from

p100 to p52 (Figure 1 C), thus confirming that non-canonical NF-κB activation is also a feature of primary cells harboring *BIRC3* variants. MAP3K14 stabilization is largely associated with *BIRC3* mutations. Indeed 7/7 cases harboring non canonical NF-κB genetic lesions showed either a strong or a slight MAP3K14 band, while, conversely, only one out of 5 cases lacking non canonical NF-κB lesion had MAP3K14 expression (p by Fisher's exact test 0.01).

MAP3K14 was genetically targeted by shRNA to test whether *BIRC3* mutated cells are addicted of its stabilization. Compared to non-targeting shRNA, the most efficient anti MAP3K14 shRNA-D resulted in a partial silencing of MAP3K14 and in a decreased NF-κB_2 processing from p100 to p52. This translated into a reduced cell viability of the *BIRC3* mutated VL51 cell line transduced with shRNA-D. This observation indicates that MAP3K14 stabilization is a vulnerability of *BIRC3* mutated cells (Figure 2). In order to test the contribution of BTK to non-canonical NF-κB signaling when it is activated through *BIRC3* mutations, *BIRC3* mutated cell lines, as well as cell lines harboring a disrupted or competent TRAF3/MAP3K14-TRAF2/BIRC3 negative regulatory complex were treated with ibrutinib at different dosage and non-canonical NF-κB signaling activation probed by immunoblotting of the NF-κB_2 processing from p100 to p52. Processing from p100 to p52 was unaffected by ibrutinib treatment in cell lines harboring *BIRC3* mutations (Figure 3) or a disrupted TRAF3/MAP3K14-TRAF2/BIRC3 negative regulatory complex consistent with the notion that *BIRC3* mutations activate non-canonical NF-κB by bypassing BTK blockade by ibrutinib.[14]

***BIRC3* mutations confer resistance to fludarabine in primary CLL cells**

We performed *in vitro* pharmacological studies on primary CLL cells to verify the vulnerabilities of *BIRC3* mutated cells. CLL cells purified from patients carrying *BIRC3* mutations were treated with increasing doses of fludarabine. Drug-induced apoptosis was compared to samples harboring *TP53* mutations, which represent a control for fludarabine resistance. CLL cells

devoid of genetic lesions on either *BIRC3* or *TP53* were adopted as a control cohort for fludarabine sensitivity. Molecular characteristic of the ex-vivo CLL cells are listed in Table S4.

BIRC3 mutated cells showed a delayed fludarabine-induced cell death, as no response was observed after 24-hour treatment, at variance with *TP53* and *BIRC3* wild type samples. At this time point, cell viability curves of *BIRC3* mutated samples were almost completely overlapping with that of *TP53* disrupted samples, which are known to be fludarabine resistant (Figure 4 A). At 48 hours, *BIRC3* mutated cells had viability that was lower than that of *TP53* mutated samples, but higher than that of *TP53* and *BIRC3* wild type samples (Figure 4 B).

In order to assess whether *BIRC3* mutations interfere with apoptosis, primary CLL cells were treated with venetoclax. Venetoclax treatment resulted in similar reduction of cell viability in *BIRC3* mutated cells, *TP53* mutated cells and *BIRC3/TP53* wild type cells (Figure 4 C,D). Such divergent sensitivity to fludarabine and venetoclax of *BIRC3* mutated CLL cells indirectly suggests that *BIRC3* mutations likely affect the upstream DNA damage response pathway rather than the downstream apoptosis among mechanisms of cell death induction.

Patients harboring *BIRC3* mutations are at risk of failing FCR

In order to confirm *in vivo* in patients that *BIRC3* mutations confer resistance to fludarabine-based chemoimmunotherapy, we correlated the *BIRC3* mutation status with PFS in FCR treated CLL. Mutational profiling was performed in 287 patients who received first line FCR. The baseline features of the study cohort were consistent with progressive, previously untreated CLL (Table 1). The median follow-up was 6.8 years, with a median PFS and OS of 4.6 and 11.7 years, respectively (Table 1) consistent with clinical trial cohorts.[15] As expected, *SF3B1* and *NOTCH1*were the most frequently mutated genes identified in 13.9% and in 13.6% of patients respectively, followed by *TP53* in 9.4% and *ATM* in 6.9% of patients. *BIRC3* was mutated in 3.1% of patients, reflecting the data reported in previous studies.[6,7,13] Overall, 154/287 (53.6%) cases harbored at least one non-synonymous somatic mutation in one of the 24 CLL genes included in our panel (range: 1-5

mutation per patient), which is consistent with the typical mutational spectrum of CLL requiring first line treatment (Figure 5; Table S5). [6,7,16]

By univariate analysis adjusted for multiple comparisons, among the genes analyzed in our panel, only *TP53* mutations (median PFS of 2.6 years; $p < 0.0001$) and *BIRC3* mutations (median PFS of 2.2 years; $p < 0.001$) (Figure 6 A) associated with significantly shorter PFS (Table 2). The PFS after FCR of *BIRC3* mutated patients was similar to that of cases harboring *TP53* disruption (Figure 6 B). Consistently, *BIRC3* mutated patients had a lower likelihood of achieving complete response (22.2%) at the end of FCR compared to *BIRC3* wild type cases (76.7%; $p=0.001$). Well-known molecular prognostic biomarkers of CLL, such as unmutated *IGHV* gene status and 17p deletion also associated with a significantly shorter PFS, supporting the representativeness of the study cohort (Table 2). By multivariate analysis including variables showing a multiplicity adjusted significant association with PFS, *BIRC3* mutations maintained an independent association with PFS, with a HR of 2.8 (95% C.I. 1.4-5.6, $p = 0.004$) (Table 2).

DISCUSSION

The results of this study provide the evidence that: *i) BIRC3* mutations associate with activation of the non-canonical NF-κB pathway and with resistance to fludarabine *in vitro*; and that *ii) BIRC3* mutated patients fail FCR chemoimmunotherapy analogous to cases harboring *TP53* disruption.

The mere presence of somatic mutations is insufficient to implicate a gene in cancer. Cancer geneticists and bioinformaticians differentiate "passengers" events, likely being randomly acquired, to distinguish them from mutations targeting candidate "cancer driver" genes, likely implicated in the tumor biology, according to a statistical definition. Any given gene is labeled as candidate "cancer driver" if it harbors somatic point mutations at a statistically significant rate or pattern in cancer samples. In CLL, more than 40 genes fulfill the statistical definition of candidate "cancer driver", including *BIRC3*, but few of them are biologically validated (i.e. *SF3B1*, *NOTCH1*, *TP53*, *ATM*, *FBXW7*).[6,7,17-20] The *BIRC3* (Baculoviral IAP Repeat Containing 3) gene codes for a protein that ubiquitinates and negatively regulates the central activating kinase of the non-canonical NF-κB pathway, namely MAP3K14 (also known as NIK).[21,22] In lymphoid malignancies, the NF-κB pathway is a pivotal and positive mediator of cell proliferation and survival.[5,23,24] In CLL, *BIRC3* mutations are absent in monoclonal B-cell lymphocytosis (MBL) patients, are rare at the time of diagnosis (3-4%), but are detectable in approximately 25% of fludarabine refractory patients.[13] In this study, we verified the biological consequences of *BIRC3* mutations by showing that they associate with activation of the non-canonical NF-κB pathway, that *BIRC3* mutated lymphoid cells are addicted of non-canonical NF-κB pathway, and that *BIRC3* mutated CLL are resistant to fludarabine both *in vitro* and in patients. It still remains to be clarified whether NF-κB activation is the only molecular pathway that causes chemo-refractoriness in *BIRC3* mutated CLL or whether other mechanisms are also involved.[24-29]

The introduction of FCR has represented a breakthrough in the management of young and fit CLL patients with an improvement in both PFS and OS compared to previous regiments. In both clinical trials and real life cohorts,[10-12] *IGHV* mutation status and *TP53* disruption sorted out as strong predictors of poor response to FCR. However, these molecular biomarkers do not fully capture all high-risk patients destined to relapse. We propose *BIRC3* mutations as a new biomarker for the identification of high-risk patients failing FCR similarly to cases harboring *TP53* disruption. If validated in independent series, *BIRC3* mutations may turn out as a new molecular predictor of FCR resistance to be use for selecting patients to be treated with novel targeted agents.

Non-canonical NF-κB activation by *BIRC3* mutations by-pass the block of BTK by ibrutinib. Consistently, NF-κB activation and cell survival is unaffected by ibrutinib in both CLL cells (our study) and mantle cell lymphoma cells.[14] If this pre-clinical evidence will be validated in ibrutinib-treated patients, *BIRC3* mutations may translate in a biomarker also for informing selection of novel agents.

REFERENCES

1. Mansouri L, Papakonstantinou N, Ntoufa S, Stamatopoulos K, Rosenquist R. NF-κB activation in chronic lymphocytic leukemia: A point of convergence of external triggers and intrinsic lesions. Semin Cancer Biol. 2016;39:40-48
2. Bonizzi G, Karin M. The two NF-kappaB activation pathways and their role in innate and adaptive immunity. Trends Immunol. 2004;25(6):280-288.
3. Oeckinghaus A, Hayden MS, Ghosh S. Crosstalk in NF-κB signaling pathways. Nat Immunol. 2011;12(8):695-708.
4. Sun SC. The noncanonical NF-κB pathway. Immunol Rev. 2012;246(1):125-140.
5. Asslaber D, Wacht N, Leisch M, Qi Y, et al. BIRC3 Expression Predicts CLL Progression and Defines Treatment Sensitivity via Enhanced NF-κB Nuclear Translocation. Clin Cancer Res. 2019;25(6):1901-1912.
6. Puente XS, Beà S, Valdés-Mas R, et al. Non-coding recurrent mutations in chronic lymphocytic leukaemia. Nature. 2015;526(7574):519-524.
7. Landau DA, Tausch E, Taylor-Weiner AN, et al. Mutations driving CLL and their evolution in progression and relapse. Nature. 2015;526(7574):525-530.
8. Hallek M, Cheson BD, Catovsky D, et al. Guidelines for diagnosis, indications for treatment, response assessment and supportive management of chronic lymphocytic leukemia. Blood. 2018;131(25):2745-2760.
9. Gaidano G, Rossi D. The mutational landscape of chronic lymphocytic leukemia and its impact on prognosis and treatment. Hematology Am Soc Hematol Educ Program. 2017;2017(1):329-337.
10. Rossi D, Terzi-di-Bergamo L, De Paoli L, et al. Molecular prediction of durable remission after first-line fludarabine-cyclophosphamide-rituximab in chronic lymphocytic leukemia. Blood. 2015;126(16):1921-1924.

11. Thompson PA, Tam CS, O'Brien SM, et al. Fludarabine, cyclophosphamide, and rituximab treatment achieves long-term disease-free survival in IGHV-mutated chronic lymphocytic leukemia. Blood. 2016;127(3):303-309.
12. Fischer K, Bahlo J, Fink AM, et al. Long-term remissions after FCR chemoimmunotherapy in previously untreated patients with CLL: updated results of the CLL8 trial. Blood. 2016;127(2):208-215.
13. Rossi D, Fangazio M, Rasi S, et al. Disruption of BIRC3 associates with fludarabine chemorefractoriness in TP53 wild-type chronic lymphocytic leukemia. Blood. 2012;119(12):2854-2862.
14. Rahal R, Frick M, Romero R, et al. Pharmacological and genomic profiling identifies NF-κB-targeted treatment strategies for mantle cell lymphoma. Nature Medicine. 2014;20(1):87-92.
15. Hallek M, Fischer K, Fingerle-Rowson G, et al. Addition of rituximab to fludarabine and cyclophosphamide in patients with chronic lymphocytic leukaemia: a randomised, open-label, phase 3 trial. Lancet. 2010;376(9747):1164-1174.
16. Stilgenbauer S, Schnaiter A, Paschka P, et al. Gene mutations and treatment outcome in chronic lymphocytic leukemia: results from the CLL8 trial. Blood. 2014;123(21):3247-3254.
17. Grossmann V, Kohlmann A, Schnittger A, et al. Recurrent ATM and BIRC3 Mutations in Patients with Chronic Lymphocytic Leukemia (CLL) and Deletion 11q22-q23. Blood. 2012;120(21):1771.
18. Rose-Zerilli MJ, Forster J, Parker H, et al. ATM mutation rather than BIRC3 deletion and/or mutation predicts reduced survival in 11q-deleted chronic lymphocytic leukemia: data from the UK LRF CLL4 trial. Haematologica. 2014;99(4):736-742.
19. Baliakas P, Hadzidimitriou A, Sutton LA, et al. Recurrent mutations refine prognosis in chronic lymphocytic leukemia. Leukemia. 2015;29(2):329-336.

20. Nadeu F, Delgado J, Royo C, et al. Clinical impact of clonal and subclonal TP53, SF3B1, BIRC3, NOTCH1, and ATM mutations in chronic lymphocytic leukemia. Blood. 2016;127(17):2122-2130.
21. Vince JE, Wong WW, Khan N, et al. IAP antagonists target cIAP1 to induce TNFalpha-dependent apoptosis. Cell. 2007;131(4):682-693.
22. Jost PJ, Ruland J. Aberrant NF-kappaB signaling in lymphoma: mechanisms, consequences, and therapeutic implications. Blood. 2007;109(7):2700-2707.
23. Raponi S, Del Giudice I, Ilari C, et al. Biallelic BIRC3 inactivation in chronic lymphocytic leukaemia patients with 11q deletion identifies a subgroup with very aggressive disease. Br J Haematol. 2019;185(1):156-159.
24. Hewamana S, Lin TT, Jenkins C, et al, The novel nuclear factor-kappaB inhibitor LC-1 is equipotent in poor prognostic subsets of chronic lymphocytic leukemia and shows strong synergy with fludarabine. Clin Cancer Res. 2008;14(24):8102-8111.
25. Hewamana S, Alghazal S, Lin TT, et al. The NF-κB subunit Rel A is associated with in vitro survival and clinical disease progression in chronic lymphocytic leukemia and represents a promising therapeutic target. Blood. 2008;111:4681–4689.
26. Beg AA, Baltimore D. An essential role for NF-κB in preventing TNF-α-induced cell death. Science. 1996;274:782–784.
27. Wang CY, Mayo MW, Baldwin AS, Jr. TNF- and cancer therapy-induced apoptosis: potentiation by inhibition of NF-κB. Science. 1996;274:784–787.
28. Webster GA, Perkins ND. Transcriptional cross talk between NF-κB and p53. Mol Cell Biol. 1999;19:3485–3495.
29. Nakanishi C, Toi M. Nuclear factor-κB inhibitors as sensitizers to anticancer drugs. Nat Rev. 2005;5:297–309

Table 1. Clinical data of FCR-treated CLL patients accordig to *BIRC3* mutational status

Characteristics	Total	Number of patients (%)	*BIRC3* mutated patients (%)	*BIRC3* wild type patients (%)
Male	N=287	198 (69.0%)	5 (55.6%)	193 (69.4%)
Female		89 (31.0%)	4 (44.4)	85 (30.6%)
Binet A	N=287	33 (11.5%)	1 (11.1%)	32 (11.5%)
Binet B-C		254 (88.5%)	8 (88.9%)	246 (88.5%)
IGHV mutated	N=280	100 (35.7%)	0 (0%)	100 (36.0%)
IGHV unmutated		180 (64.3%)	9 (100%)	171 (61.5%)
17p deletion	N=274	13 (4.7%)	0 (0%)	13 (4.7%)
No 17p deletion		261 (95.3%)	9 (100%)	252 (90.6%)
11q deletion	N=273	47 (17.2%)	5 (55.6%)	42 (15.1%)
No 11q deletion		226 (82.8%)	4 (44.4)	222 (79.9%)
13q deletion	N=273	111 (40.7%)	3 (33.3%)	108 (38.8%)
No 13q deletion		162 (50.3%)	6 (66.6%)	156 (56.1%)
Trisomy 12	N=272	50 (18.4%)	4 (44.4%)	46 (16.5%)
No Trisomy 12		222 (81.6%)	5 (55.6%)	217 (78.1%)

Median Follow-up (years)	6.8
Median PFS (years)	4.6
PFS % (7-years)	31.0%
Median OS (years)	11.7
OS % (7-years)	75.5%

PFS, progression free survival; OS, overall survival; *IGHV*, immunoglobulin heavy variable gene.

Table 2. Univariate and multivariate analysis of PFS

	Univariate analysis					Multivariate analysis				Internal bootstrapping validation			
Characteristics	**7-y PFS (%)**	**Median PFS (y)**	**95% CI**	***P***	***P****	**HR**	**LCI**	**UCI**	***P***	**HR**	**LCI**	**UCI**	**Bootstrapping selection (%)**
Binet A	40.3%	4.5	2.4-6.6	0.356	-	-	-	-	-	-	-	-	-
Binet B-C	30.0%	4.6	3.8-5.4			-	-	-		-	-	-	
***IGHV* mutated**	49.3%	6.5	3.8-9.2	<0.001	0.003	-	-	-	0.001	-	-	-	98.8%
***IGHV* unmutated**	23.0%	3.9	3.5-4.4			1.8	1.3	2.6		1.9	1.3	2.7	
No 11q deletion	33.4%	5.0	4.2-5.9	0.025	0.700	-	-	-	-	-	-	-	-
11q deletion	13.9%	3.6	2.4-4.9			-	-	-		-	-	-	
No 17p deletion	33.0%	4.8	4.1-5.6	<0.0001	<0.0001	-	-	-	<0.0001	-	-	-	99.5%
17p deletion	nr	1.1	0-2.6			4.0	2.2	7.5		4.9	2.5	9.8	
***TP53* Wild type**	33.8%	5.4	4.3-5.8	<0.0001	<0.001	-	-	-	0.030	-	-	-	73.3%
***TP53* Mutated**	nr	2.8	2.0-3.5			1.7	1.1	2.8		1.8	1.1	3	
***BIRC3* Wild type**	32.2%	4.8	4.1-5.6	<0.001	0.005	-	-	-	0.004	-	-	-	91.1%
***BIRC3* Mutated**	nr	2.2	0.9-3.5			2.8	1.4	5.6		3.4	1.6	7.3	
***EGR2*Wild type**	31.5%	4.7	3.9-5.4	0.015	0.420	-	-	-	-	-	-	-	-
***EGR2*Mutated**	nr	1.5	0-3.8			-	-	-		-	-	-	
***ATM* Wild type**	32.5%	4.8	4.1-5.6	0.029	0.812	-	-	-	-	-	-	-	-
***ATM* Mutated**	nr	3.2	2.4-4.1			-	-	-		-	-	-	

P, P-value; *P**, Bonferroni correction; PFS, progression free survival; CI, confidence interval; HR, hazard ratio; LCI, lower confidence interval; UCI, upper confidence interval; *IGHV*, immunoglobulin heavy variable gene; nr, not reached

FIGURE LEGENDS

Figure 1: Non-canonical NF-κB pathway is active in *BIRC3* mutated CLL cell lines and primary samples. (A) Disposition of *BIRC3* mutations across the protein. The mutations identified by Landau *et al.*[6], Puente *et al.*[7] and from public CLL mutation catalogue (COSMIC v85) are plotted in grey. Individual *BIRC3* mutations identified in the current studied cohort and in our previous study[13] are plotted in red. **(B)** Western blot analysis of BIRC3 protein expression and NF-κB_2 activation and processing in the SMZL cell lines SSK41, VL51 and in the CLL cell line MEC1, carrying wild-type or disrupted *BIRC3*. The MAVER-1 and Z-138 cell lines were used as positive controls of non-canonical NF-κB activation, harboring genetic activation of non-canonical NF-kB signaling. The JEKO-1 and HEK 293T cell lines were used as negative controls for non-canonical NF-κB signalling. α-actin was used as a loading control. Color codes indicate the gene status in each cell lines. The aberrant BIRC3 band expressed in MEC1 and VL51 cell lines correspond in size to the predicted BIRC3-truncated protein, encoded by the mutant allele. **(C)** Western blot analysis showing BIRC3 expression and NF-kB_2 processing in purified primary tumor cells from 5 CLL and SMZL patients carrying wild-type or disrupted *BIRC3*. Color codes indicate the gene status in each cell lines. The aberrant *BIRC3* bands in patients 09321, 14462 and 12603 correspond in size to the predicted BIRC3-truncated protein encoded by the mutant allele. α-actin was used as a loading control. **(D)** Western blot of whole cell extract, cytoplasmic or nuclear fractions of the SMZL and CLL cell lines probed for the NF-κB_2 subunits p100 and p52. The MAVER-1 and Z-138 cell lines served as positive controls while the JEKO-1 and HEK 293T cell lines were used as negative controls. ß-tubulin and BRG1 served as controls for the purity of the cytoplasmic and nuclear fractionations, respectively. **(E)** GSEA enrichment score and distribution of non-canonical NF-κB target genes along the rank of transcripts differentially expressed in the SMZL cell lines SSK41, VL51 and in the CLL cell line MEC1. The JEKO-1 cell line was used as negative control.

(F) Validation of non-canonical NF-κB target genes expression in the same SMZL and CLL cell lines as determined by quantitative real-time RT-PCR. Changes of genes expression were normalized to *GAPDH* expression; relative quantities were $\log_2$ normalized to control samples (MCL cell line JEKO-1).

Figure 2: Knockdown of MAP3K14 by RNA interference in VL51 cells. (A) Western blot analysis for MAP3K14 expression and for NF-κB_2 processing of p100 to p52. **(B)** VL51 cells viability assessed by trypan blue after transduction with lentiviral vectors expressing the shRNAD_MAP3K14 (in red), a scrambled shRNA (in blu), and in non transfected cells (in green).

Figure 3: Non-canonical NF-κB pathway is not switched off by ibrutinib in *BIRC3* mutated cell lines. Western blot showing p100/p52 expression in **(A)** MEC1 and **(B)** VL51 cell lines that harbors *BIRC3* mutations. **(C)** MAVER-1 and **(D)** Z-138 cell lines, known to be affected by non-canonical NF-κB pathway gene mutations and resistant to ibrutinib were used as positive controls. **(E)** JEKO-1 cell line, known to be devoid of NF-κB pathway gene mutations and sensitive to ibrutinib was used as negative control. All cell lines were treated with different concentrations of ibrutinib for 72 and 96 hours.

Figure 4: Responses of primary cells lines to fludarabine and venetoclax. Viability of *BIRC3* mutated (n = 6 patients, red line), *TP53* mutated (n = 8 patients, black line) and wild type (n = 7 patients, blue line) primary CLL cells treated with different concentrations of fludarabine for **(A)** 24 hours and **(B)** 48 hours and of venetoclax for **(C)** 24 hours and **(D)** 48 hours The pairwise p values have been listed in the tables below the respective figures. M, mutated; WT, wild type; NT, not treated.

Figure 5. Mutational profile of the FCR-treated cohort. Case-level mutational profiles of 287 patients FCR-treated patients. Each column represents one tumor sample, each row represents one gene. The fraction of tumors with mutations in each gene is plotted on the right. The number and type of mutations in each patient is plotted above the heat map. Mutations are highlighted in red. *IGHV* mutational status, 17p deletion and 11q deletion are plotted in the bottom of the heatmap.

Figure 6. Kaplan-Meier estimates of progression free survival in *BIRC3* mutated patients. **(A)** Cases harboring *BIRC3* mutations are represented by the red line. Cases wild type for this gene are represented by the blue line. **(B)** Cases harboring *BIRC3* mutations are represented by the red line. Cases harboring *TP53* disruption (including *TP53* mutation and/or 17p deletion) are represented by the yellow line. Patients devoid of *BIRC3* mutation and *TP53* disruption are represented by the blue line. The Log-rank statistics p values are indicated adjacent curves.

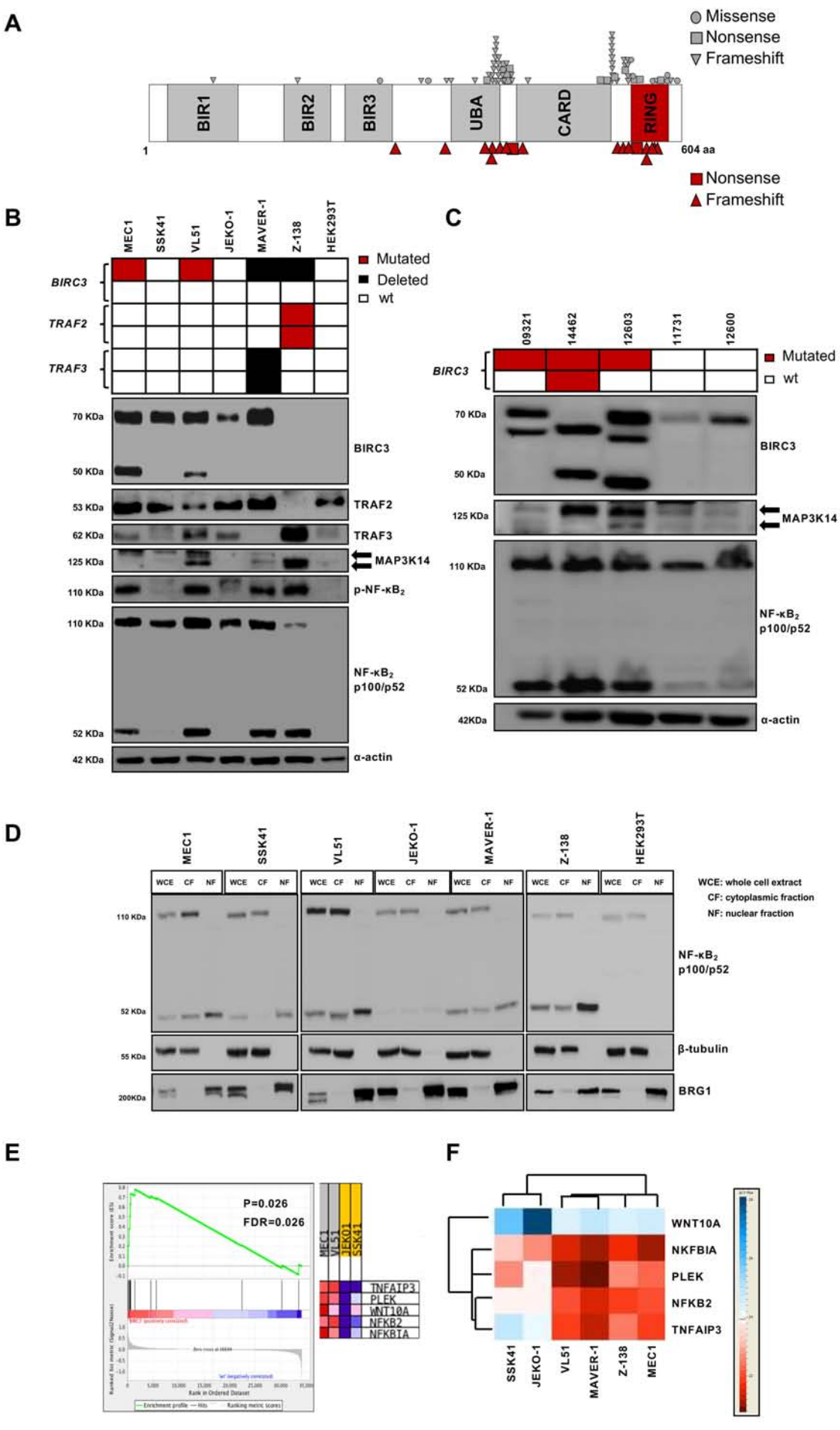
A
Missense
Nonsense
Frameshift
BIR1
BIR2
BIR3
UBA
CARD
RING
1
604 aa
Nonsense
Frameshift
B
MEC1
SSK41
VL51
JEKO-1
MAVER-1
Z-138
HEK293T
Mutated
Deleted
wt
BIRC3
TRAF2
TRAF3
70 KDa
50 KDa
53 KDa
62 KDa
125 KDa
110 KDa
110 KDa
52 KDa
42 KDa
BIRC3
TRAF2
TRAF3
MAP3K14
p-NF-κB2
NF-κB2 p100/p52
α-actin
C
09321
14462
12603
11731
12600
Mutated
wt
BIRC3
70 KDa
50 KDa
125 KDa
110 KDa
52 KDa
42KDa
BIRC3
MAP3K14
NF-κB2 p100/p52
α-actin
D
MEC1
SSK41
VL51
JEKO-1
MAVER-1
Z-138
HEK293T
WCE
CF
NF
WCE: whole cell extract
CF: cytoplasmic fraction
NF: nuclear fraction
110 KDa
52 KDa
55 KDa
200KDa
NF-κB2 p100/p52
β-tubulin
BRG1
E
P=0.026
FDR=0.026
MEC1
VL51
JEKO1
SSK41
TNFAIP3
PLEK
WNT10A
NFKB2
NFKBIA
Rank in Ordered Dataset
Enrichment profile
Hits
Ranking metric scores
F
WNT10A
NKFBIA
PLEK
NFKB2
TNFAIP3
SSK41
JEKO-1
VL51
MAVER-1
Z-138
MEC1

Figure 1

Figure 2

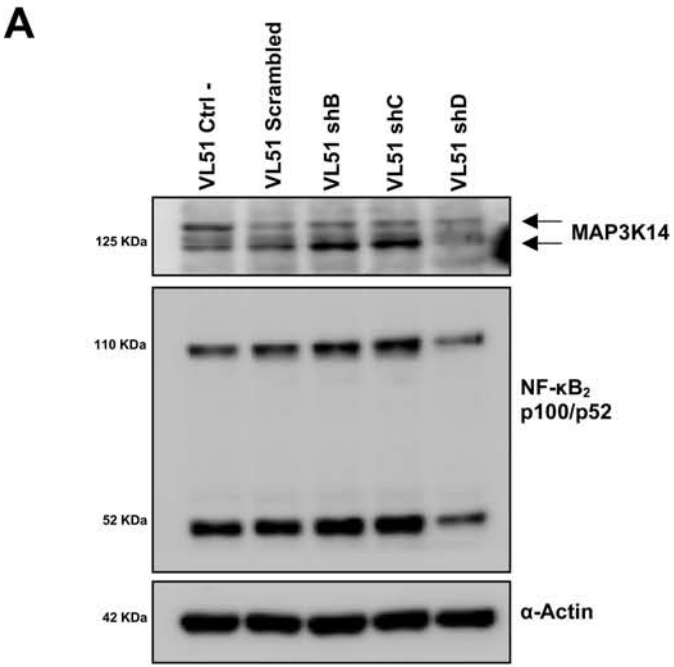
A
VL51 Ctrl -
VL51 Scrambled
VL51 shB
VL51 shC
VL51 shD
125 KDa
MAP3K14
110 KDa
NF-κB2
p100/p52
52 KDa
42 KDa
α-Actin

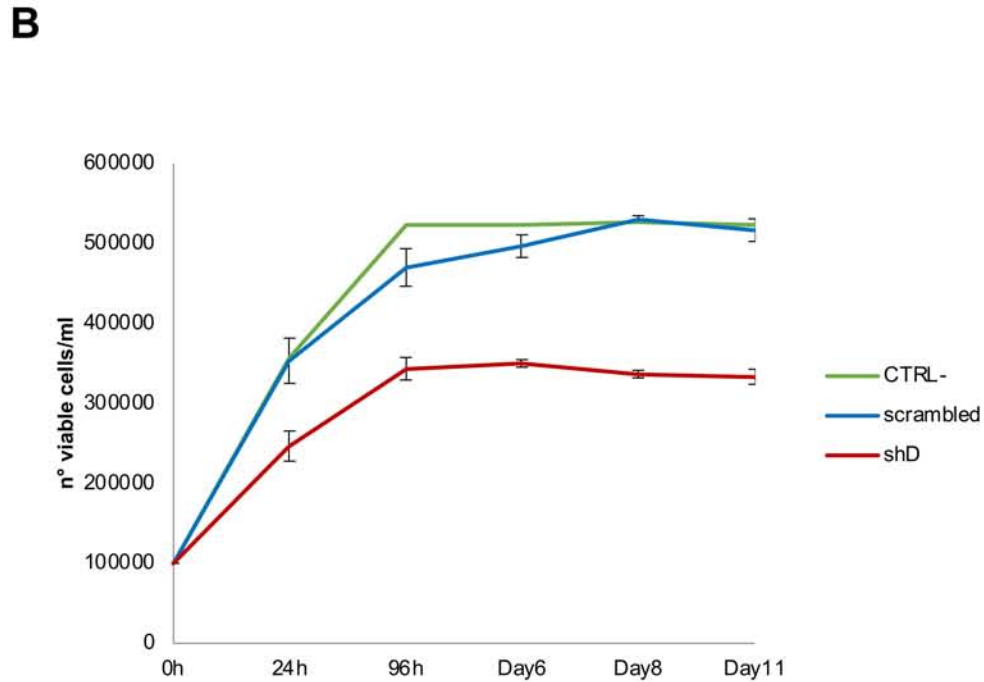
B
n° viable cells/ml
600000
500000
400000
300000
200000
100000
0
0h
24h
96h
Day6
Day8
Day11
CTRL-
scrambled
shD

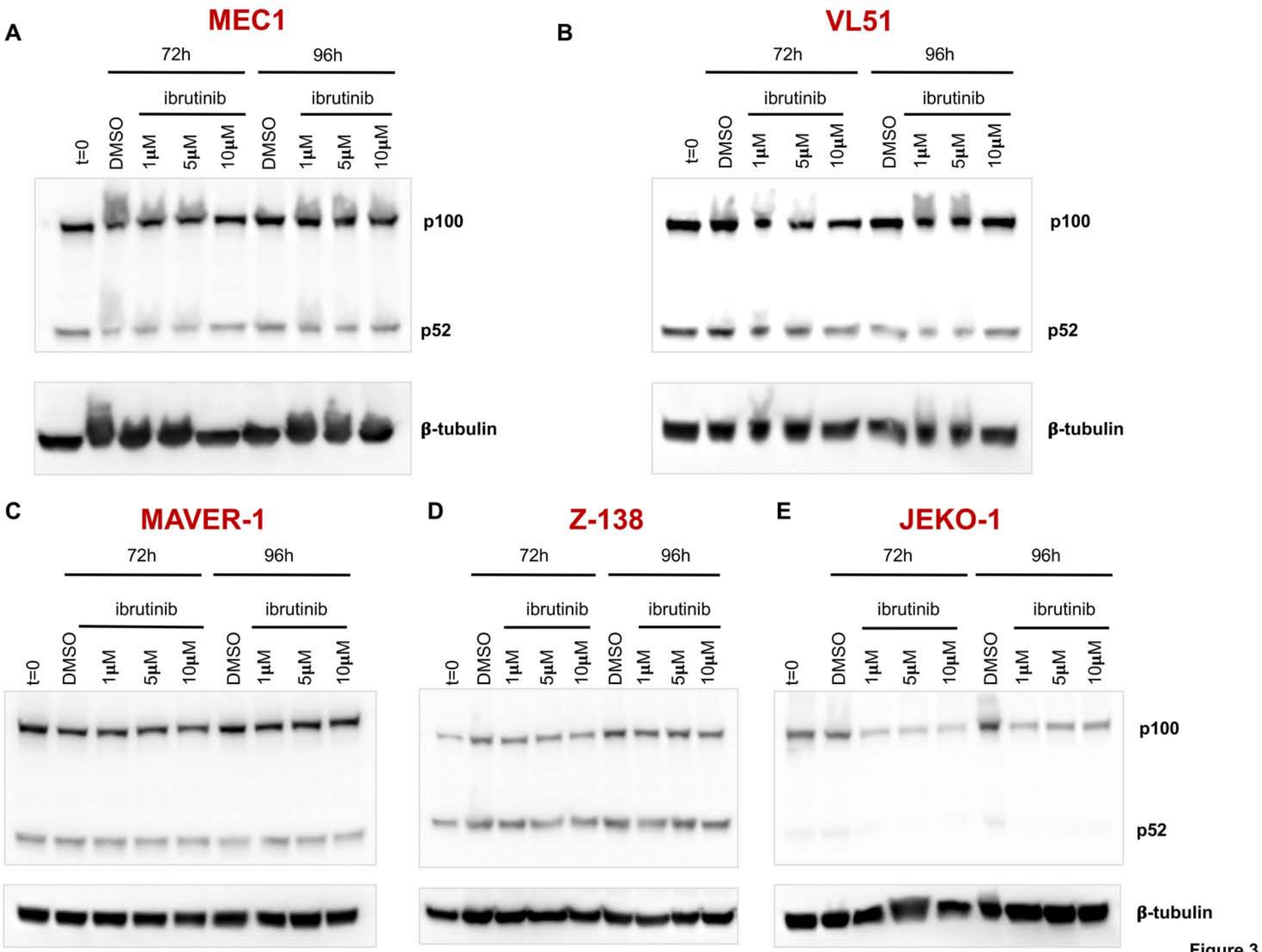
A
MEC1
72h
96h
ibrutinib
ibrutinib
t=0
DMSO
1μM
5μM
10μM
DMSO
1μM
5μM
10μM
p100
p52
β-tubulin
B
VL51
72h
96h
ibrutinib
ibrutinib
t=0
DMSO
1μM
5μM
10μM
DMSO
1μM
5μM
10μM
p100
p52
β-tubulin
C
MAVER-1
72h
96h
ibrutinib
ibrutinib
t=0
DMSO
1μM
5μM
10μM
DMSO
1μM
5μM
10μM
D
Z-138
72h
96h
ibrutinib
ibrutinib
t=0
DMSO
1μM
5μM
10μM
DMSO
1μM
5μM
10μM
E
JEKO-1
72h
96h
ibrutinib
ibrutinib
t=0
DMSO
1μM
5μM
10μM
DMSO
1μM
5μM
10μM
p100
p52
β-tubulin

Figure 3

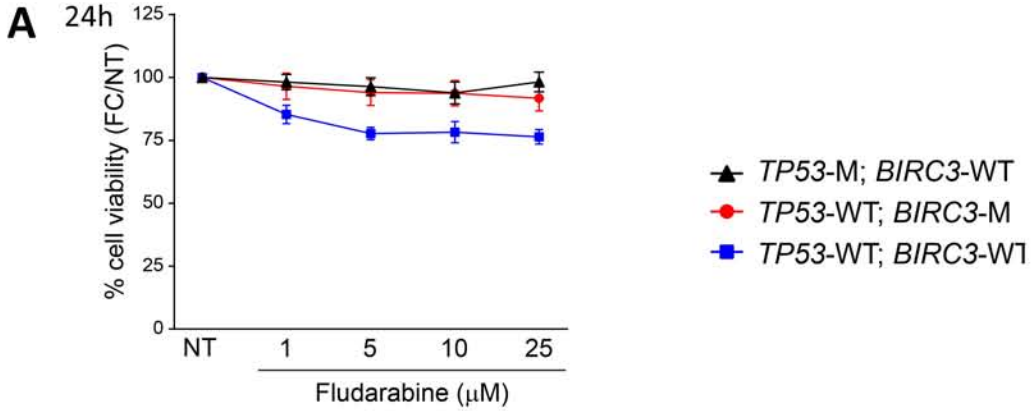

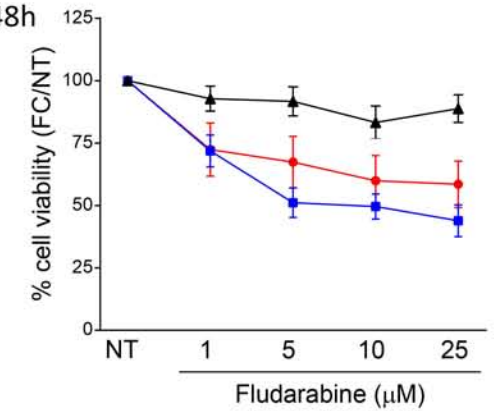

	NT	Fludarabine 1mM	Fludarabine 5mM	Fludarabine 10mM	Fludarabine 25mM
TP53-M vs. *BIRC3*-M	p>0.9999	p=0.9447	p=0.8923	p=0.9997	p=0.4311
TP53-M vs. WT	p>0.9999	p=0.0567	p=0.0031	p=0.0078	p=0.0005
BIRC3-M vs. WT	p>0.9999	p=0.1117	p=0.0112	p=0.0115	p=0.0184

	NT	Fludarabine 1mM	Fludarabine 5mM	Fludarabine 10mM	Fludarabine 25mM
TP53-M vs. *BIRC3*-M	p>0.9999	p=0.0837	p=0.0309	p=0.0320	p=0.0053
TP53-M vs. WT	p>0.9999	p=0.0737	p=0.0001	p=0.0004	p<0.0001
BIRC3-M vs. WT	p>0.9999	p=0.9982	p=0.2043	p=0.4756	p=0.2742

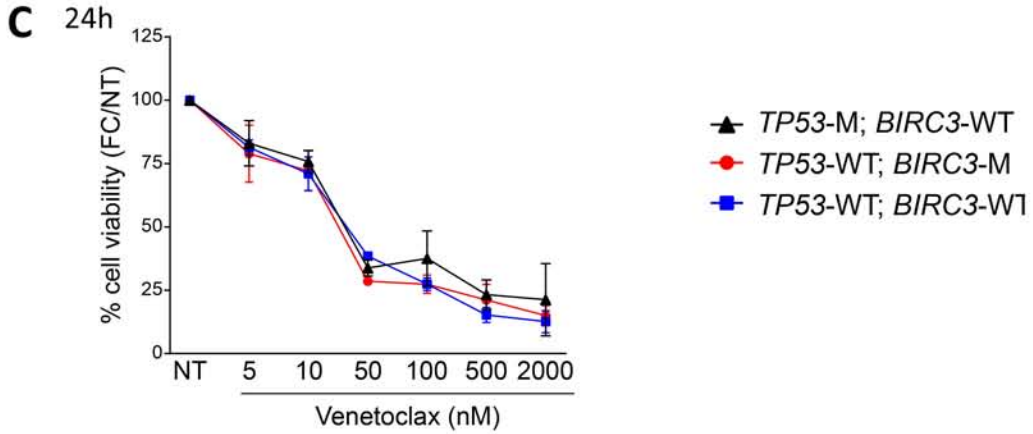

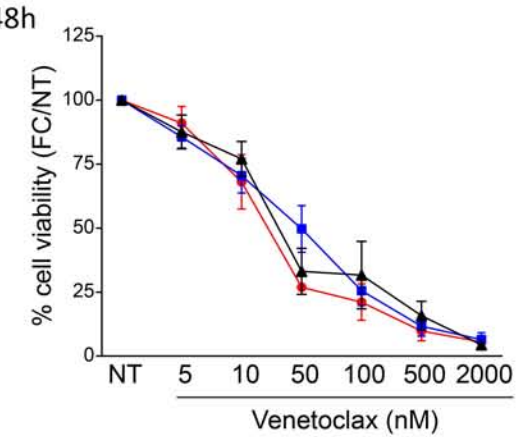

	NT	Venetoclax 5nM	Venetoclax 10nM	Venetoclax 50nM	Venetoclax 100nM	Venetoclax 500nM	Venetoclax 2000nM
TP53-M vs. *BIRC3*-M	p>0.9999	p=0.8947	p=0.8655	p=0.8875	p=0.3674	p=0.9572	p=0.7936
TP53-M vs. WT	p>0.9999	p=0.9832	p=0.7777	p=0.9071	p=0.3703	p=0.4943	p=0.6441
BIRC3-M vs. WT	p>0.9999	p=0.9594	p=0.9852	p=0.6507	p>0.9999	p=0.7095	p=0.9504

	NT	Venetoclax 5nM	Venetoclax 10nM	Venetoclax 50nM	Venetoclax 100nM	Venetoclax 500nM	Venetoclax 2000nM
TP53-M vs. *BIRC3*-M	p>0.9999	p=0.9512	p=0.5282	p=0.9119	p=0.4524	p=0.7524	p=0.7524
TP53-M vs. WT	p>0.9999	p=0.9800	p=0.6789	p=0.3778	p=0.7438	p=0.8597	p=0.8597
BIRC3-M vs. WT	p>0.9999	p=0.8844	p=0.9547	p=0.2959	p=0.8518	p=0.9722	p=0.9722

Figure 4

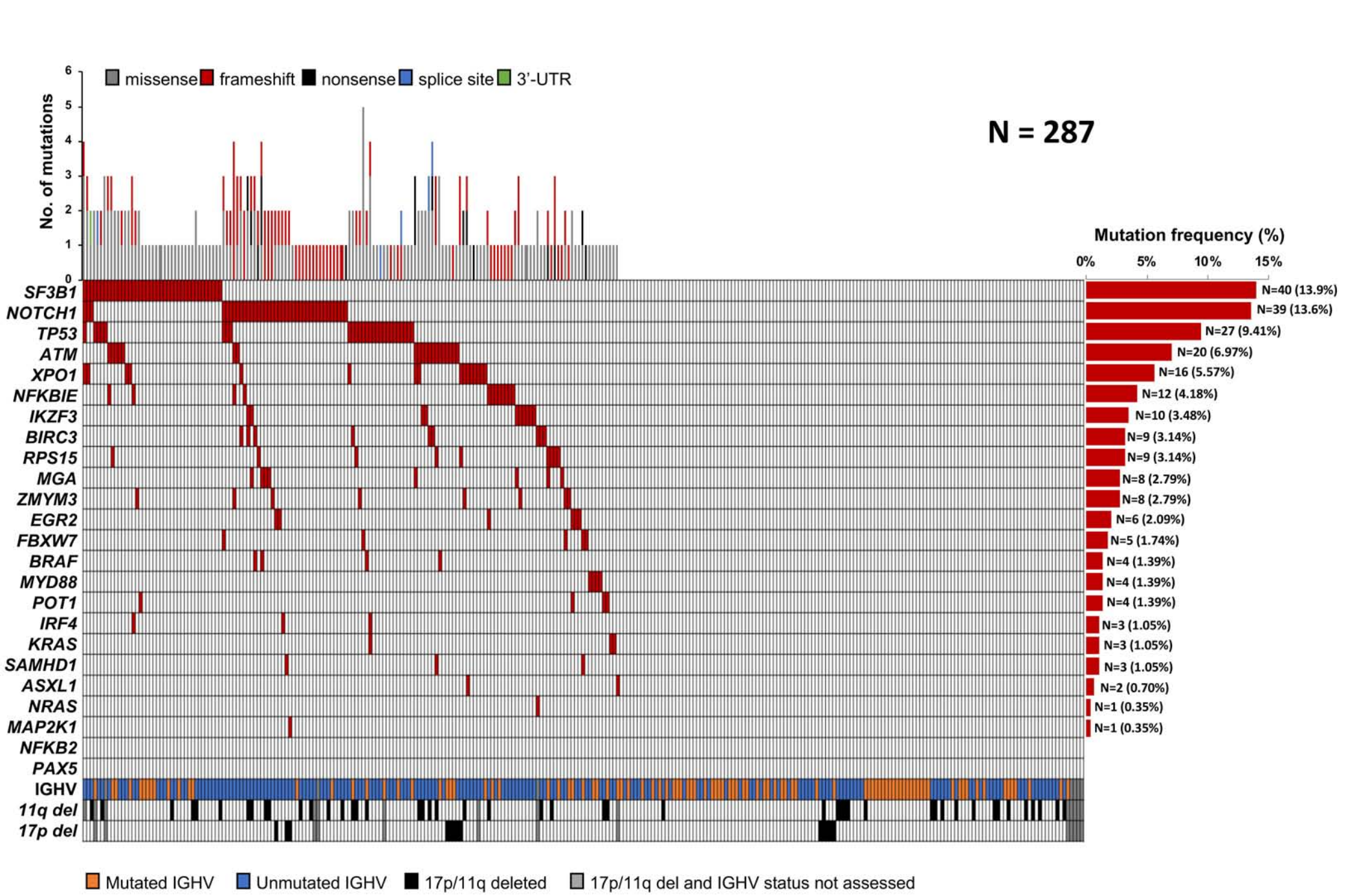
missense
frameshift
nonsense
splice site
3'-UTR
No. of mutations
0
1
2
3
4
5
6
N = 287
Mutation frequency (%)
0%
5%
10%
15%
SF3B1
NOTCH1
TP53
ATM
XPO1
NFKBIE
IKZF3
BIRC3
RPS15
MGA
ZMYM3
EGR2
FBXW7
BRAF
MYD88
POT1
IRF4
KRAS
SAMHD1
ASXL1
NRAS
MAP2K1
NFKB2
PAX5
IGHV
11q del
17p del
N=40 (13.9%)
N=39 (13.6%)
N=27 (9.41%)
N=20 (6.97%)
N=16 (5.57%)
N=12 (4.18%)
N=10 (3.48%)
N=9 (3.14%)
N=9 (3.14%)
N=8 (2.79%)
N=8 (2.79%)
N=6 (2.09%)
N=5 (1.74%)
N=4 (1.39%)
N=4 (1.39%)
N=4 (1.39%)
N=3 (1.05%)
N=3 (1.05%)
N=3 (1.05%)
N=2 (0.70%)
N=1 (0.35%)
N=1 (0.35%)
Mutated IGHV
Unmutated IGHV
17p/11q deleted
17p/11q del and IGHV status not assessed

Figure 5

Figure 6

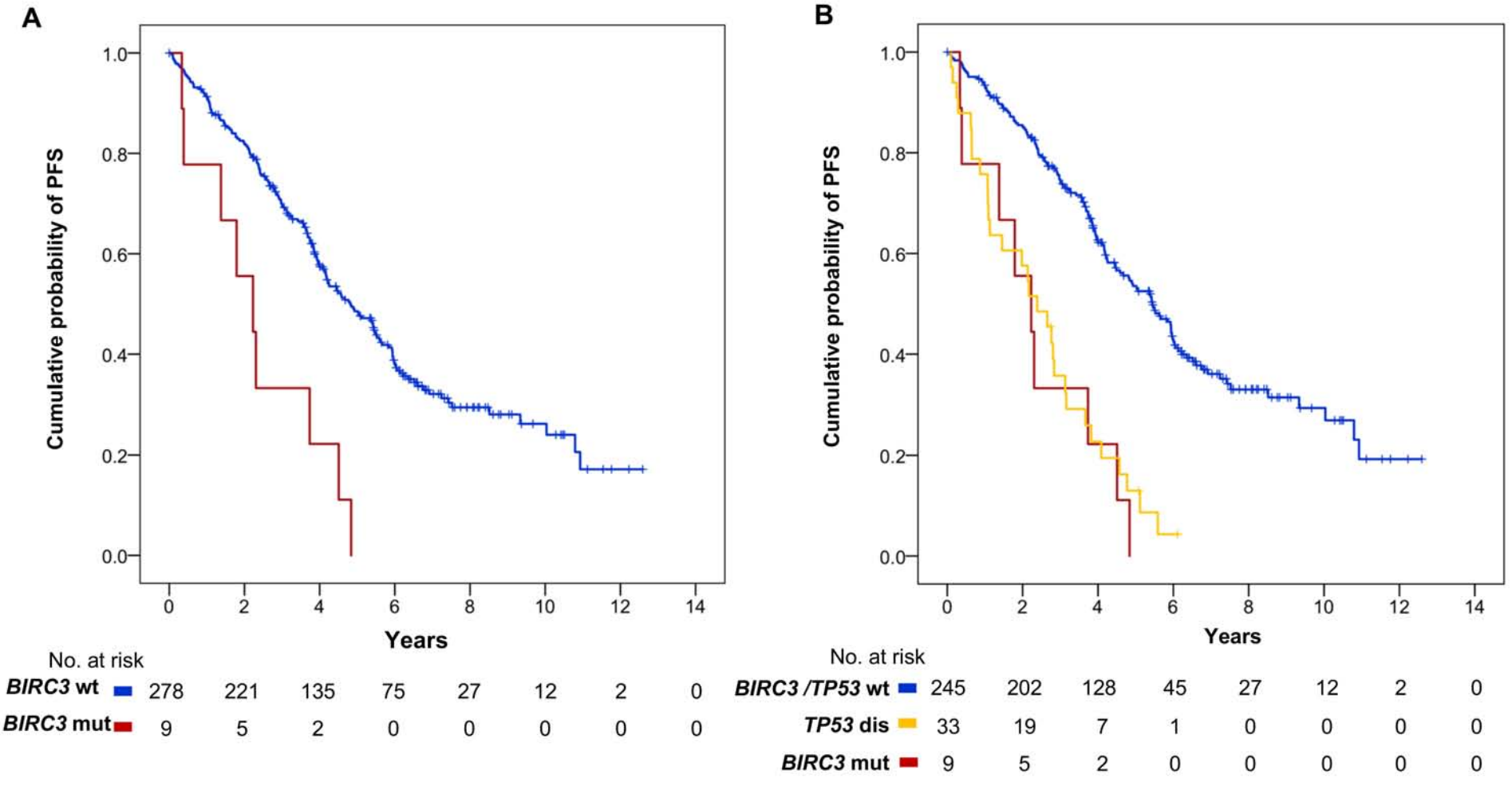
A
Cumulative probability of PFS
1.0
0.8
0.6
0.4
0.2
0.0
0
2
4
6
8
10
12
14
Years
No. at risk
BIRC3 wt 278 221 135 75 27 12 2 0
BIRC3 mut 9 5 2 0 0 0 0 0
B
Cumulative probability of PFS
1.0
0.8
0.6
0.4
0.2
0.0
0
2
4
6
8
10
12
14
Years
No. at risk
BIRC3 /TP53 wt 245 202 128 45 27 12 2 0
TP53 dis 33 19 7 1 0 0 0 0
BIRC3 mut 9 5 2 0 0 0 0 0

SUPPLEMENTARY APPENDIX

BIOLOGICAL AND CLINICAL IMPLICATIONS OF *BIRC3* MUTATIONS IN CHRONIC LYMPHOCYTIC LEUKEMIA

Fary Diop,[1*] Riccardo Moia,[1*] Chiara Favini,[1] Elisa Spaccarotella,[1] Lorenzo De Paoli,[1] Alessio Bruscaggin,[2] Valeria Spina,[2] Lodovico Terzi-di-Bergamo,[2] Francesca Arruga[3], Chiara Tarantelli[4], Clara Deambrogi,[1] Silvia Rasi,[1] Ramesh Adhinaveni,[1] Andrea Patriarca,[1] Simone Favini,[1] Sruthi Sagiraju,[1] Clive Jabangwe[1], Ahad A. Kodipad,[1] Denise Peroni,[1] Francesca R. Mauro,[5] Ilaria Del Giudice,[5] Francesco Forconi,[6,7] Agostino Cortelezzi,[8] Francesco Zaja,[9] Riccardo Bomben,[10] Francesca Maria Rossi, [10] Carlo Visco,[11] Annalisa Chiarenza,[12] Gian Matteo Rigolin,[13] Roberto Marasca,[14] Marta Coscia,[15] Omar Perbellini,[16] Alessandra Tedeschi,[17] Luca Laurenti,[18] Marina Motta,[19] David Donaldson,[20] Phil Weir,[20] Ken Mills,[21] Patrick Thornton,[22] Sarah Lawless[20], Francesco Bertoni[4], Giovanni Del Poeta,[23] Antonio Cuneo,[13] Antonia Follenzi,[24] Valter Gattei,[10] Renzo Luciano Boldorini,[25] Mark Catherwood,[20] Silvia Deaglio,[3] Robin Foà,[5] Gianluca Gaidano[1°] and Davide Rossi[2°]

*FR and RM equally contributed to the study; °GG and DR equally contributed

[1]Division of Hematology, Department of Translational Medicine, Amedeo Avogadro University of Eastern Piedmont, Novara, Italy; [2]Institute of Oncology Research and Oncology Institute of Southern Switzerland, Bellinzona, Switzerland; [3]Department of Medical Sciences, University of Turin & Italian Institute for Genomic Medicine, Turin, Italy; [4]Università della Svizzera italiana, Institute of Oncology Research, Bellinzona, Switzerland; [5]Hematology, Department of Cellular Biotechnologies and Hematology, Sapienza University, Rome, Italy; [6]Cancer Sciences Unit, Southampton Cancer Research UK and National Institute for Health Research Experimental Cancer Medicine Centre, University of Southampton, Southampton, United Kingdom; [7]Division of Hematology, University of Siena, Siena, Italy; [8]Department of Hematology Oncology, Foundation IRCCS Ca' Granda Ospedale Maggiore Policlinico and University of Milan, Milan, Italy; [9]Clinica Ematologica, DAME, University of Udine, Udine, Italy; [10]Clinical and Experimental Onco-Hematology Unit, Centro di Riferimento Oncologico, Istituto di Ricovero e Cura a Carattere Scientifico (IRCCS), Aviano, Italy; [11]Department of Cell Therapy and Hematology, Ospedale San Bortolo, Vicenza, Italy; [12]Division of Hematology, Azienda Ospedaliera Universitaria Policlinico-OVE, Catania, Italy; [13]Hematology Section, Azienda Ospedaliero Universitaria Arcispedale S. Anna, University of Ferrara, Ferrara, Italy; [14]Division of Hematology, Department of Oncology and Hematology, University of Modena and Reggio Emilia, Modena, Italy; [15]Division of Hematology, Azienda Ospedaliero Universitaria Città della Salute e della Scienza and University of Turin, Turin, Italy; [16]Section of Hematology, Department of Medicine, University of Verona, Verona, Italy; [17]Department of Oncology/Haematology, Niguarda Cancer Center, Niguarda Ca Granda Hospital, Milan, Italy; [18]Fondazione Policlinico Universitario A. Gemelli, Rome, Italy; [19]Department of Hematology, Spedali Civili, Brescia, Italy; [20]Clinical Haematology, Belfast City Hospital, Belfast Health and Social Care Trust, Belfast, Northern Ireland; [21]Centre for Cancer Research and Cell Biology (CCRCB), Queen's University Belfast, Belfast, Northern Ireland, United Kingdom; [22]Department of Haematology, Beaumont Hospital, Dublin; [23]Department of Hematology, Tor Vergata University, Rome, Italy; [24]Department of Health Sciences, University of Eastern Piedmont Amedeo Avogadro, Novara, Italy; Department of Pathology, University of Eastern Piedmont Amedeo Avogadro, Novara, Italy.

SUPPLEMENTARY METHODS

Cell studies
The human CLL cell line MEC1, the SMZL cell lines SSK41, VL51, and the MCL cell lines MAVER-1, Z-138 and JEKO-1 were cultured under standard conditions in RPMI-1640 with L-glutamine supplemented with 10% fetal calf serum, 100 U/ml penicillin and 100 U/ml streptomycin (Sigma Aldrich). Human HEK-293T cells were maintained in Iscove's Modified Dulbecco Medium (IMDM) supplemented with 10% fetal calf serum, 100 U/ml penicillin, 100 U/ml streptomycin and 2mM L-glutamine (Sigma Aldrich) under identical conditions.
Three primary cells samples known to harbor heterozygous inactivating mutations of *BIRC3* were included in the experiments. Two *BIRC3* wild type cases were used as controls.

Western blot analysis
The entire non-canonical NF-κB pathway was assessed using the following specific primary antibodies: anti-BIRC3 (Cell Signaling, #3130), anti-TRAF2 (Cell Signaling, #4712), anti-TRAF3 (Cell Signaling, #4729), anti-MAP3K14 (Cell Signaling, #4994), anti-Phospho-NF-κB2 p100 (Cell Signaling, #4810), anti-NF-κB2 p100/p52 (Cell Signaling, #4882). Anti-β-actin (Sigma Aldrich, #A2066) was used as loading control. The Qproteome Nuclear Protein Kit (Qiagen) was used according to the manufacturer's instructions to isolate nuclear proteins from cells. Anti-β-tubulin (Sigma Aldrich, #T5201) and anti-BRG1 (G-7) (Santa Cruz Biotechnology, #17796) were used as controls for the purity of the cytoplasmic and nuclear fractions, respectively. Horseradish peroxidase-conjugated goat anti-mouse (LI-COR, #926-80010) or anti-rabbit (LI-COR, #926-80011) antibodies were used to highlight binding by enhanced chemiluminescence with the Clarity Western ECL Substrate (Biorad). Image acquisition and densitometric analyses were performed using the Molecular Imager Gel Doc XR System and the Quantity One software (Biorad).

RNA extraction and gene expression profiling
Total RNA was extracted from exponentially growing cell lines by TRIzol reagent (Life Technologies), and retro-transcribed using the Reverse Transcription Kit (Applied Biosystems). Quantitative real-time PCR (qRT-PCR) was conducted with the Step One Plus apparatus (Step One software 2.0; Applied Biosystems) using commercially available TaqMan Gene expression assays (TNFAIP3: Hs00234713_m1; NFKB2: Hs00174517_m1; NFKBIA: Hs00153283_m1; NFKBIE: Hs00234431_m1; PLEK: Hs00950975_m1; WNT10: Hs00228741_m1; IL2RG: Hs00953624_m1; RELB: Hs00232389_m1; MALT1: Hs01120052_m1) (BIRC3: Hs00985031_g1) (Life Technologies). Reactions were done in triplicate from the same cDNA (technical replicates). The comparative CT method (ΔΔCT) was used to calculate relative expression levels of the gene under analysis, using GAPDH (Hs03929097_g1) as internal references.

Knockdown of MAP3K14 by RNA interference
Lentiviruses expressing 3 short hairpin RNAs (shRNAs) targeting MAP3K14, as well as the scrambled shRNA, were produced and cloned into the BamHI/HindIII cloning sites of the pGFP-C-shLenti vectors (OriGene Technologies). Within the 5'-LTR and 3'-LTR regions, each pGFP-C-shLenti vector contains an shRNA expression cassette driven by an U6 promoter, a puromycin resistance marker driven by a SV40 promoter and a GFP driven by a CMV promoter. The shRNA expression cassette consists of 29 bp target-gene-specific sequence, a 7 bp loop, and another 29 bp reverse complementary sequence, followed by a TTTTTT termination sequence. The HEK293T cell line was co-transfected with expression (3 different pGFP-C-MAP3K14-shLenti or pGFP-C-non-effective-shLenti) vectors and adjuvant vectors (pMDL, REV and VSV-G). Fluorescence microscope was utilized to check the expression of the GFP in the transfected HEK293T cell line. After virus titration, the VL51 cell line was infected with lentiviruses harboring the shRNAs against MAP3K14 and the scrambled through a spinoculation protocol. After four days, infected cells were monitored by flow cytometry for the expression of the GFP and were selected by puromycin (1.5 μg/mL).

Inhibitor studies
Cells were put under starvation in RPMI 0.1% FBS 24h before treatment. Then they were seeded at 8000 cells per well in a 96-well U-bottom plate and treated with 1 μM, 5 μM and 10 μM of Ibrutinib (PCI-32765, Selleckchem) or vehicle (DMSO). Relative growth was determined by a Cell-Titer Glo (CTG) Luminescent Cell Viability Assay (Promega) 72h and 96h after treatment, according to the manufacturer's instructions and luminescence was quantified using a Victor X (PerkinElmer) multilabel reader. Treatments were done in triplicate (biological replicates).

***In vitro* drug responses in primary CLL cells**
Leukemic cells were purified using Ficoll-Hypaque (Sigma Aldrich) from peripheral blood (PB) of CLL patients. Staining with CD19 and CD5 confirmed that in all samples leukemic cells were >90%. Patients were then divided into *BIRC3* mutated (MUT) or wild-type (WT). *TP53* mutated samples (and *BIRC3* WT) were selected as positive control (i.e., cells intrinsically resistant to therapies). Cells were cultured in RPMI 10% FCS (200 μl, all reagents from Sigma) at a density of 5x106/ml and both dose- and time-dependent responses were analyzed. Specifically, CLL cells were exposed to fludarabine) for 24-48 hours. Fludarabine was used at 1-5-10-25 μM and venetoclax at 5-10-50-100-500-2000 nM.

Apoptosis assay
Drug-induced apoptosis was measured using the eBioscience™ Annexin V Apoptosis Detection Kit APC (ThermoFisher) following the manufacturer's instruction. Data were acquired using a FACSCanto II cytofluorimeter (BD Biosciences) and processed with DIVA v6.1.3 and FlowJo Version 9.01 (TreeStar).

FCR treated patients
The study was designed as a retrospective observational analysis from a multicenter cohort of 287 (275 with complete clinical and molecular data) untreated CLL receiving first-line therapy with FCR in 17 different hematological centers. The following biological material was collected: *i)* 280 tumor genomic DNA (gDNA) and 7 tumor RNA isolated from peripheral blood (PB) before treatment start; and *ii)* paired germline gDNA from saliva from 14 cases. Normal gDNA from 22 healthy donors was also used to set the experimental background of the deep next generation sequencing (NGS) approach. Tumor and normal gDNA was extracted according to standard procedures[1].Tumor RNA was extracted according to the TRIzol Reagent protocol (Ambion Life Technologies). The clinical database was updated in April 2018. Patients provided informed consent in accordance with local Institutional Review Board requirements and the Declaration of Helsinki. The study was approved by the Ethical Committee of the Ospedale Maggiore della Carità di Novara associated with the Amedeo Avogadro University of Eastern Piedmont (study number CE 67/14).

Cancer personalized profiling by deep sequencing (CAPP-seq)
A targeted resequencing gene panel [2] was designed to include: *i)* coding exons plus splice site of 24 CLL genes known to be implicated in CLL pathogenesis and/or prognosis; *ii)* 3'UTR of *NOTCH1*; and *iii)* enhancer and promoter region of *PAX5* [3,4] (size of the target region: 66627bp). Tumor and germline gDNA were quantified using the Quant-iT™ PicoGreen dsDNA Assay kit (ThermoFisher Scientific) and 400 ng were sheared through sonication (Covaris M220 focused-ultrasonicator) before library construction to obtain 200-bp fragments. The size of the DNA fragments was checked using the Bioanalyzer (Agilent Technologies). The NGS libraries for gDNA were constructed using the KAPA Library Preparation Kit (Kapa Biosystems) and NGS libraries for RNA were constructed using RNA Hyper Kit (Roche) following the manufacturer's instructions. Hybrid selection was performed with the custom SeqCap EZ Choice Library (Roche NimbleGen). Multiplexed libraries (n = 10 per run) were sequenced using 300-bp paired-end runs on a MiSeq sequencer (Illumina).

Bioinformatic pipeline for variant calling after CAPP-seq
Initially, FASTQ sequencing reads were deduped. We deduped FASTQ sequencing reads from gDNA by utilizing the FastUniq v1.1 software, that collapses as duplicate reads only those fragments (read pairs) with 100% sequence identity that also share genomic coordinates. The same approach was also used to dedupe germline gDNA and normal gDNA from 22 healthy donors, to avoid the introduction of biases in variant calling due to the application of different deduplication protocols. Then, the deduped FASTQ sequencing reads were locally aligned to the hg19 version of the human genome assembly using the BWA v.0.6.2 software with the default setting, and sorted, indexed and assembled into a mpileup file using SAMtools v.1. The aligned read families were processed with mpileup using the parameters -A -d 10000000. For cases provided with paired germline gDNA, single nucleotide variations and indels were called in tumor gDNA vs germline gDNA, respectively, with the somatic function of VarScan2 using the parameters min-coverage 1 --min-coverage-normal 1 --min-coverage-tumor 1 --min-var-freq 0--min-freq-for-hom 0.75 --somatic-p-value 0.05 --min-avg-qual 20 --strand-filter 1 --validation 1. For cases lacking paired germline gDNA, single nucleotide variations and indels were called in tumor gDNA using the CNS function of VarScan2 using the parameters --min-coverage 0 --min-readge 2 --min-avg-qual 20 --min-var-freq 0 --min-freq-for-hom 0.75 --p-value 0.05 --strand-filter 1 --output-vcf 1 --variants 0. The variants called by VarScan 2 were annotated using the SeattleSeq Annotation 138 tool by using the default setting. Variants annotated as SNPs according to dbSNP 138 (with the exception of *TP53* variants that were manually curated and scored as SNPs according to the IARC TP53 database), intronic variants mapping > 2 bp before the start or after the end of coding exons, and synonymous variants were then filtered out. The following strict post-processing filters were then applied to the remaining variants to further improve variant call confidence. To filter out variants below the base-pair resolution background frequencies in gDNA across the selector, for cases provided with paired germline gDNA, the Fisher's exact test was used to test whether the frequency of the variant called by VarScan 2 was significantly higher from that called in the corresponding paired germline gDNA, after adjusting for multiple comparisons by Bonferroni test [multiple comparisons corrected p threshold = 0.00000018761163, corresponding to alpha of 0.05/(66627 x 4 alleles per position]. Accordingly, variants represented in > 10 reads of the paired germline and/or variants with a somatic p value from VarScan2 > 0.00000018761163 were no further considered. To filter out systemic sequencing errors, a database containing all germline and normal gDNA background allele frequencies was assembled. Based on the assumption that all background allele fractions follow a normal distribution, for both cases provided with paired germline gDNA and cases lacking paired gDNA, a Z-test was employed to test whether a given variant in the tumor gDNA differed significantly in its frequency from typical germline or normal gDNA background at the same position in all the other germline and normal gDNA samples, after adjusting for multiple comparisons by Bonferroni test [multiple comparisons corrected p threshold = 0.00000018761163, corresponding to alpha of 0.05/(66627 x 4 alleles per position]. Variants that

did not pass this filter were no further considered. Variant allele frequencies for the resulting candidate mutations and the background error rate were visualized using IGV.

Statistical analysis

Progression free survival (PFS) was the primary endpoint and was measured from date of treatment start to date of progression according to IWCLL-NCI guidelines (event), death (event) or last follow-up (censoring). Overall survival (OS) was measured from date of initial presentation to date of death from any cause (event) or last follow-up (censoring). Survival analysis was performed by Kaplan-Meier method and compared between strata using the Log-rank test. A false discovery rate approach was used to account for multiple testing, and adjusted p-values were calculated using the Bonferroni correction. A maximally selected rank statistic was used to determine the optimal cut-off for variant allele frequency (VAF) based on the Log-rank statistics. A cut-off of 3% of VAF was set for *TP53* mutations and of 10% for all the other genes. The adjusted association between exposure variables and PFS was estimated by Cox regression. Internal validation of the multivariate analysis was performed using a bootstrap approach to estimate means and confidence intervals of hazard ratios, and percentage of selection for each variable in the model. The number of bootstrap samples used was 1000. Apoptosis assays were analyzed using the two-way ANOVA test. All statistical tests were two-sided. Statistical significance was defined as p value < 0.05. The analysis was performed with the Statistical Package for the Social Sciences (SPSS) software v.24.0 (Chicago, IL), with R statistical package 3.1.2 and with GraphPad version 7 (GraphPad Software Inc).

SUPPLEMENTARY TABLES ON EXCEL FILE ONLY

Table S1. Target region (Excel file)

Table S2. Target region with ≥1000X and ≥2000X coverage (Excel file)

Table S3. 11q deletion, 17p deletion and *TP53* mutational status of tumor cell lines and primary CLL cells (Excel file)

Table S4. Primary cell lines divided into *BIRC3/TP53* mutated or wild-type (WT). (Excel file)

Table S5. Somatic non-synonymous mutations discovered in tumor samples (Excel file)

SUPPLEMENTARY REFERENCES

1. Miller SA, Dykes DD, Polesky HF. A simple salting out procedure for extracting DNA from human nucleated cells. *Nucleic Acids Res*. 1988;16(3):1215.
2. Newman AM, Bratman SV, To J, Wynne JF, et al. An ultrasensitive method for quantitating circulating tumor DNA with broad patient coverage. *Nat Med*. 2014;20(5):548-554.
3. Landau DA, Tausch E, Taylor-Weiner AN, et al. Mutations driving CLL and their evolution in progression and relapse. *Nature*. 2015;526(7574):525-530.
4. Puente XS, Beà S, Valdés-Mas R, et al. Non-coding recurrent mutations in chronic lymphocytic leukaemia. *Nature*. 2015;526(7574):519-524.